Development and Verification of a Tropical Cyclone Intensity Estimation Method Reflecting the Variety of TRMM/TMI Brightness Temperature Distribution

Tomoaki Sakuragi[1], Shunsuke Hoshino[1, 2], Naoko Kitabatake[1]

[1]Typhoon Research Department, Meteorological Research Institute, JMA
[2]Present Affiliation: Aerological Observatory, JMA

Abstract

This paper presents an objective method for the estimation of maximum tropical cyclone (TC) wind speeds using 10, 19, 21, 37 and 85 GHz channel Tropical Rainfall Measurement Mission (TRMM) Microwave Imager (TMI) brightness temperature (TB) data collected between 1998 and 2008. TC structures are represented by parameterized TB distribution, and TC cases are classified into 10 clusters using the k-means method of cluster analysis. A regression equation is determined for each cluster to allow estimation of maximum TC wind speeds in the cluster. The results of verification for the period from 2009 to 2012 showed a root mean square error (RMSE) of 6.26 m/s, which is comparable to that of the Dvorak technique. A method to complement TRMM data coverage is also introduced for cases in which coverage exceeds 85%. This increases the frequency of estimation by 15%.

1. Introduction

Tropical cyclones (TCs) are generated and intensify in data-sparse regions over the sea in the tropics. A geostationary meteorological satellite observing a wide region over the globe at a relatively high temporal resolution (e.g., intervals of 30 minutes) is essential for monitoring such storms. The Dvorak technique (Dvorak 1975, 1984) is widely used as a primary tool in the estimation of TC intensity. As this approach is based on the classification of cloud patterns in infrared and/or visible imagery, it can lead to overestimation/underestimation for the intensity of TCs covered by opaque cirrus clouds in visible and infrared observation. For instance, the central dense overcast (CDO) sometimes covers the eye of the TC, and its intensity may be underestimated as a result.

Observation using microwave sensors on board orbital satellites enables detection of convection below the CDO, thereby helping to improve TC intensity estimation by providing information complementary to the Dvorak technique.

Several studies to support the estimation of TC intensity with satellite-borne microwave sensors have also been conducted. Hoshino and Nakazawa (2007) (hereafter HN07) developed a method for objective estimation of maximum TC wind speeds using Tropical Rainfall Measure Mission (TRMM) Microwave Imager (TMI) brightness temperature (TB) data. They defined regression equations using parameters from TB data and estimated maximum wind speeds. Yoshida et al. (2011) applied a similar method to TB data from another orbital satellite (Aqua/AMSR-E; operation discontinued in 2011) and estimated TC intensity.

Both HN07 and Yoshida et al. (2011) assumed an axi-symmetric structure typical of a mature TC in TB distribution, which is often unsuitable for TCs in the early and decaying stages. Kiku (2011) demonstrated that the accuracy of TC intensity estimation was improved by using several specific regression equations from the 10 introduced by Yoshida et al. (2011). Against such a background, the present study involved the development of a method for TC intensity estimation taking the variety of TRMM/TMI TB distribution into account using cluster analysis. Kitabatake et al. (2013) described the methodology in detail. This paper gives an outline of the method and several examples of estimation.

Section 2 details the estimation method, including information on TRMM/TMI TB data, classification via cluster analysis, regression equations relating TB data with maximum winds in the best track data, and verification of estimation. Section 3 introduces a method to complement TB distribution near the TC center as a way of increasing estimation frequency. Section 4 covers several cases of estimation and includes related discussion. Section 5 provides a summary and remarks.

2. Development of the TC intensity estimation method

2.1 Parameterization of TC structure using TRMM/TMI TB data

To improve the previously proposed method, regression equations enabling the estimation of maximum TC wind speeds in the western North Pacific were computed in a way similar to that proposed by HN07 using TRMM/TMI 1B11 TB data from the GSFC DAAC website (http://daac.gsfc.nasa.gov) and maximum wind speeds in the best track data from the RSMC Tokyo-Typhoon Center. For calculation of the regression equations, 1,370 observation cases between 1998 and 2008 were used.

The major difference between the proposed method and that of HN07 is its employment of asymmetric components relative to the direction of TC motion for parameter calculation using TRMM/TMI TBs. The parameter calculation regions are

illustrated in Fig. 1a, which shows a circle with the radius of 0.25° and two annuli with the radii of 0.25–0.5° and 0.5–1.0°. Additional two outer annular regions between the radii of 1° and 2° is divided into four regions defined as forward (F), backward (B), left (L) and right (R) relative to the TC motion. Thus, TB data are parameterized for 11 regions. Figure 1b shows example parameter calculation regions. The mean, minimum, maximum and ratio of pixels exceeding the TB threshold were calculated as parameters in a way similar to that of HN07. Computation was performed for vertical and horizontal polarized data from the 10, 19, 21 and 37 GHz channels and for the Polarized Corrected Temperature (PCT) of the 37 and 85 GHz channels. Eventually, 457 parameters were calculated for each observation case (see Kitabatake et al. (2013) for details).

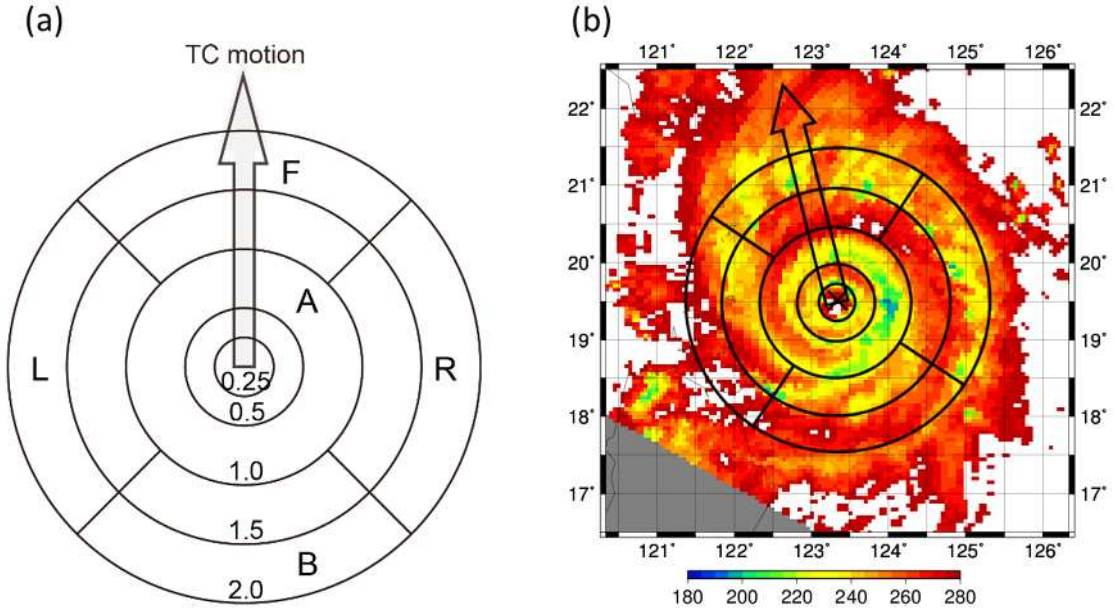

Figure 1. (a) Parameter calculation regions. The center of the concentric circles corresponds to the TC center, and the numbers indicate radial length. (b) Example of parameter calculation regions. This image shows PCT85 data for TC Songda (1102) at 0709 UTC 27 May 2011.

2.2 Cluster analysis of observed TC cases

Using the 457 parameters calculated, the 1,370 TC cases were classified into 10 clusters using the k-means method. Table 1 shows the numbers and characteristics of cases classified into the 10 clusters, and Fig. 2 shows composite PCT85 figures for the clusters.

Figure 3 shows classification correspondence determined using the proposed cluster

analysis and that obtained using the Dvorak technique applied in JMA's operational analysis. It can be seen that Clusters 0 (CL0), CL1 and CL9 include a considerable number of eye patterns, whereas most of the instances in CL2 show a shear pattern, which is inactive among Dvorak cloud patterns.

Table 1. Numbers of observed TC cases (N) and cloud pattern characteristics deduced from brightness temperature distribution for each cluster (CL). Clusters with axisymmetric brightness temperature distribution are shown in italics.

CL	N	Cloud pattern characteristic
0	*139*	*Symmetric with a small distinct eye*
1	*166*	*Symmetric with an indistinct eye*
2	84	Unorganized and inactive
3	*154*	*Small and symmetric*
4	154	Clouds over the storm center and in the left-forward quadrant
5	142	Clouds in the left-forward quadrant with an eye
6	120	Clouds behind the storm center
7	90	Clouds behind a large indistinct eye
8	124	Clouds in the right-forward quadrant
9	197	Clouds in the right-forward quadrant with a large distinct eye
all	1370	

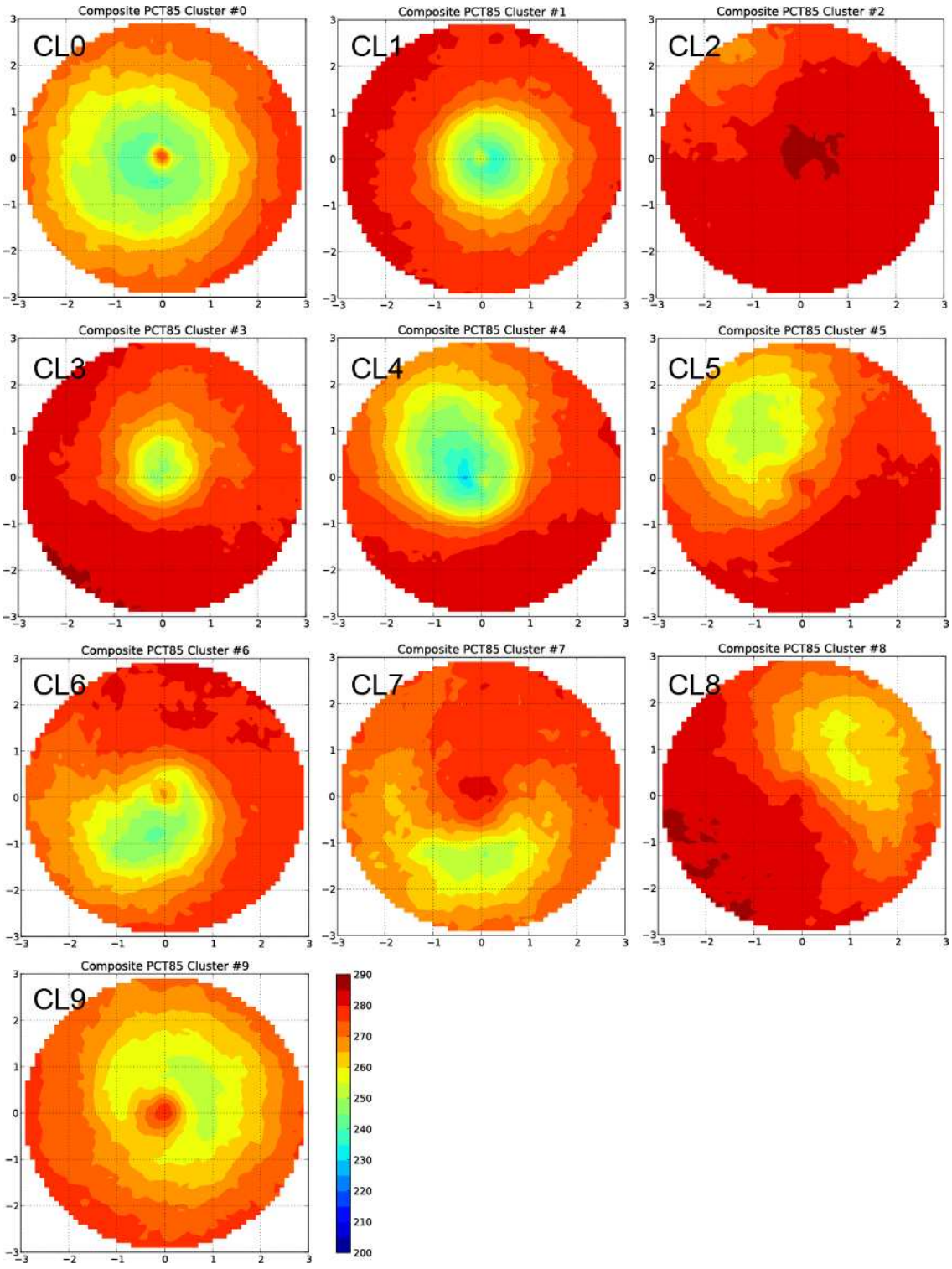

Figure 2. Composites of PCT85 data relative to storm motion within 3 degrees of latitude from the TC center for each cluster. Storm motion is upward in each panel.

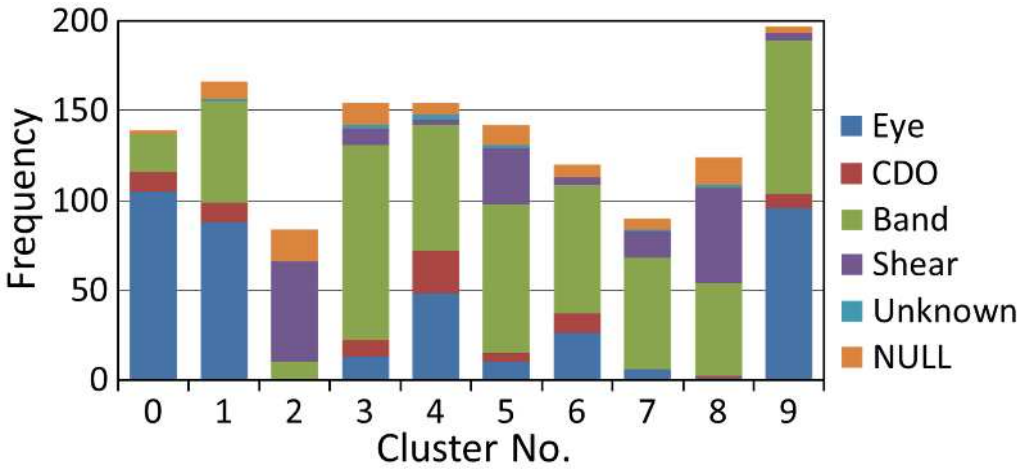

Figure 3. Dvorak cloud pattern frequency for each cluster from 1998 to 2008. "NULL" is for cases in which JMA performed no operational Dvorak analysis, e.g., after extratropical transition of the TC.

2.3 Regression analysis to relate TB parameters to TC intensity

For each cluster, a regression equation was defined using 5 to 7 of the 457 TB parameters as explanatory variables and the maximum wind speed from the best track data as an explained variable. The estimated maximum wind speed v_e is described as

$$v_e = d + \sum_{m=1}^{M} a_m P_m \qquad (m = 1, 2, \ldots M,\ M=5,6,7)\ , \qquad (1)$$

where P_m is the selected TB parameter. The coefficients a_m and d were calculated as shown in Table 2. The P_m naming convention is similar to that of HN07 except for the third parameter name group indicating the computation region. For example, Q150200R represents the quadrant on the right side relative to TC motion between the radii of 1.5 and 2.0° (see Fig. 1a).

It should be noted that the maximum wind speed is undefined in the TC best track data for a considerable number of cases including tropical depressions (< 34 kt) and storms that transform into extratropical cyclones, and these cases cannot be used for regression analysis. Cases where TB data was missing in regions for the parameter calculation were also excluded. As a result, data from 749 cases arising between 1998 and 2008 were used for the regression analysis, while 1,370 were used for the cluster

analysis. The black dots in Fig. 4 show the 749 estimates in comparison with the best track maximum wind speeds. The RMSE is 4.48 m/s (Table 3).

Table 2. Parameters and coefficients of the regression equation (Eq. (2) in the text) for each cluster (CL).

CL	d	P_1	a_1	P_2	a_2	P_3	a_3
0	-33.88	TB10V_AREA230_A025050A	0.268	TB19H_MIN_A025050A	0.0912	TB19H_MIN_Q150200R	0.211
1	-102.89	TB10V_AREA230_C025A	0.0917	TB19H_MIN_C025A	0.346	TB19H_MIN_A050100A	0.213
2	57.23	TB37H_MAX_Q150200R	0.0417	TB37H_AREA215_A025050A	-0.123	TB37H_AREA215_A050100A	0.192
3	-59.04	TB10V_MAX_Q100150R	0.171	TB19H_MEAN_A025050A	0.135	PCT85_MIN_Q150200R	0.0689
4	-84.99	TB10V_AREA230_C025A	0.0909	TB19H_MIN_A050100A	0.226	PCT85_MEAN_Q100150F	-0.155
5	73.11	TB19H_AREA190_A050100A	0.208	TB37H_MEAN_Q150200R	0.183	PCT37_MIN_A025050A	-0.306
6	-42.42	TB10V_AREA230_A025050A	0.157	TB19H_AREA190_A050100A	0.313	TB21V_AREA275_A025050A	0.136
7	-83.99	TB19V_MIN_Q100150B	0.247	TB21V_AREA255_C025A	0.109	TB37H_MEAN_Q100150R	0.228
8	-37.06	TB37H_MIN_Q100150F	0.152	TB37H_MAX_A025050A	0.0793	TB37H_AREA195_A025050A	0.0758
9	-59.13	TB10H_MIN_Q150200L	0.164	TB10V_AREA205_C025A	0.0896	TB19H_MEAN_A050100A	0.233

Table 2. (Cont.)

CL	P_4	a_4	P_5	a_5	P_6	a_6	P_7	a_7
0	TB19V_AREA270_A025050A	-0.197	TB37V_AREA260_A050100A	0.158	PCT85_AREA255_A050100A	0.154	N/A	N/A
1	TB19H_MIN_Q100150F	0.152	TB37H_MIN_C025A	-0.262	PCT85_MEAN_C025A	0.209	N/A	N/A
2	TB37V_MAX_A050100A	-0.145	PCT37_AREA265_C025A	-0.0566	PCT85_MIN_Q150200L	-0.0214	N/A	N/A
3	PCT85_AREA255_A025050A	0.160	PCT85_AREA270_C025A	0.0690	PCT85_AREA270_A025050A	-0.198	N/A	N/A
4	PCT85_MIN_Q100150F	0.0918	PCT85_MIN_Q100150B	0.0301	PCT85_MAX_C025A	0.328	PCT85_AREA270_A025050A	-0.107
5	PCT37_AREA265_A050100A	-0.0894	PCT85_MEAN_Q100150F	-0.0956	PCT85_MIN_A025050A	0.0520	PCT85_AREA270_C025A	0.0548
6	TB37H_MIN_A050100A	0.127	PCT85_MEAN_Q100150B	0.150	PCT85_MIN_C025A	-0.0732	N/A	N/A
7	TB37V_MIN_Q100150B	-0.246	PCT85_MEAN_Q100150R	0.177	N/A	N/A	N/A	N/A
8	PCT37_AREA265_C025A	-0.177	PCT85_MIN_A025050A	0.0351	PCT85_MIN_Q100150L	0.0453	N/A	N/A
9	PCT85_MIN_A050100A	0.0453	PCT85_MIN_Q150200F	0.0517	N/A	N/A	N/A	N/A

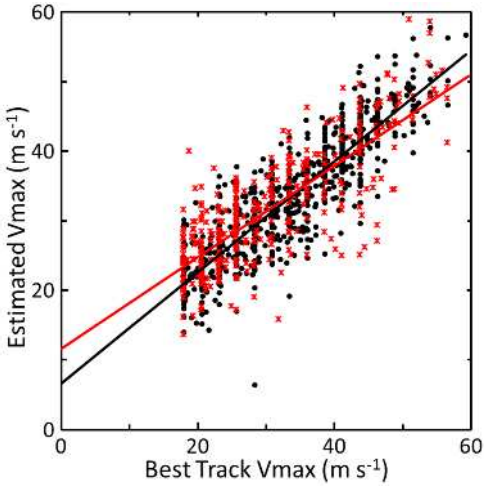

Figure 4. Scatter plots and regression lines for the best track maximum wind speed (Vmax) and estimated Vmax values. Black dots and red asterisks represent 1998 – 2008 and 2009 – 2012, respectively.

Table 3. Statistical verification of maximum wind speed estimates in comparison with those of the best track data. Figures in the "r" column show the coefficient of correlation between estimated maximum wind speed and the best track maximum wind speed.

Period	N	Bias (σ) (m/s)	RMSE (m/s)	r
1998 – 2008	749	-0.18 (4.48)	4.48	0.88
2009 – 2012	341	0.99 (6.18)	6.26	0.80

2.4 Estimation of TC intensity

By applying the above method, TC intensity was estimated for 341 cases arising between 2009 and 2012. First, the TB parameters were calculated for each of the observation case, which were then classified into the appropriate cluster using the parameters obtained. Finally, the maximum wind speed was calculated using the regression equation for the cluster into which the TC was classified. The results of such estimation for the 341 cases are shown by the red asterisks in Fig. 4, and the related statistics are presented in Table 3. The RMSE is 6.26 m/s, which is larger than that for the cases between 1998 and 2008. The estimation error is less than 10 m/s in 90.0% of all cases and less than 5 m/s in 60.1% of cases. The estimates also correlate well with the best track maximum winds.

It should be noted that the maximum wind speeds estimated using the Dvorak

technique in Koba et al. (1990) also include errors from 7 to 12 kt, which is a level comparable to that of the proposed method.

3. Complement to TRMM data coverage

As mentioned in Subsection 2.3, the observed cases with little TRMM/TMI data coverage were excluded from regression equation calculation for the period 1998 – 2008 and from estimation validation for the period 2009 – 2012. This exclusion reduces the number of opportunities for TC intensity estimation. To increase the frequency of such estimation, lacking TRMM data coverage is artificially compensated before estimation. The complement and estimation are performed as described below.

First, the parameters are calculated as described in Subsection 2.1. Although several parameters may remain undefined due to missing data coverage, the observed case can be classified into one of 10 clusters using the method outlined in Subsection 2.2. In the next step, the median for the period from 1998 to 2008 is substituted for each undefined parameter. Finally, estimation is performed using the regression equation described in Subsection 2.3. Several cases in which this procedure seems to work well are presented in Section 4.

Cases in which data coverage is significantly lacking may be classified incorrectly, which can result in erroneous intensity estimates. Figure 5 shows an example of TC Chaba (0416). It exhibits a distinct eye and an axisymmetric structure in infrared imagery, and is likely to be classified into a cluster characterized by axisymmetric structures (e.g., CL0). However, it is practically classified into CL7, and its estimated maximum wind speed is 26.31 m/s, whereas that based on the best track data is 43.77 m/s. Assuming classification into CL0, the maximum wind speed is estimated as 44.25 m/s. This suggests that a significant lack of data coverage may be poorly complemented using the above procedure, which may lead to significant estimation errors. Thus, the use of cases with a relatively significant lack of TB data coverage, excluding those with a more significant lack, is assumed to improve the accuracy and frequency of TC intensity estimation.

To examine the efficiency of the complement procedure, the relationship between data coverage and misclassification was investigated. First, cases in which the difference between the estimated maximum wind speed and that of the best track data exceeded 10 m/s from 1998 to 2012 were selected. Those in which TC-associated convections within 2° of the center were partially missing due to a lack of data coverage were then chosen for a total of 86 cases. Based on subjective judgment with reference to geostationary satellite infrared imagery, those considered to have been classified into the wrong

cluster were then defined as misclassifications. The gray bars in Fig. 6 denote the ratio of potentially misclassified cases to those with a large estimation error accompanied by a lack of TB data coverage. It can be seen that most of the large-error cases in which data coverage was less than 85% were viewed as misclassifications. Meanwhile, the ratio of potential misclassifications is quite small when data coverage is 85% or more, suggesting that large estimation errors are probably not attributable to misclassification due to a lack of data coverage. Accordingly, maximum wind speeds are estimated after application of the complement to cases in which data coverage exceeds 85%.

From 1998 to 2012, 167 cases had at least one undefined parameter due to a lack of data coverage despite coverage of 85% or more. Figure 7 compares the estimates and the best track data. The bias and RMSE are 1.01 m/s and 5.88 m/s, respectively.

As detailed in Section 2, 749 and 341 cases for 1998 – 2008 and 2009 – 2012, respectively, were suitable for the proposed estimation method (Table 3) after those with a lack of data coverage were excluded. The data coverage complement increases estimation frequency by about 15%.

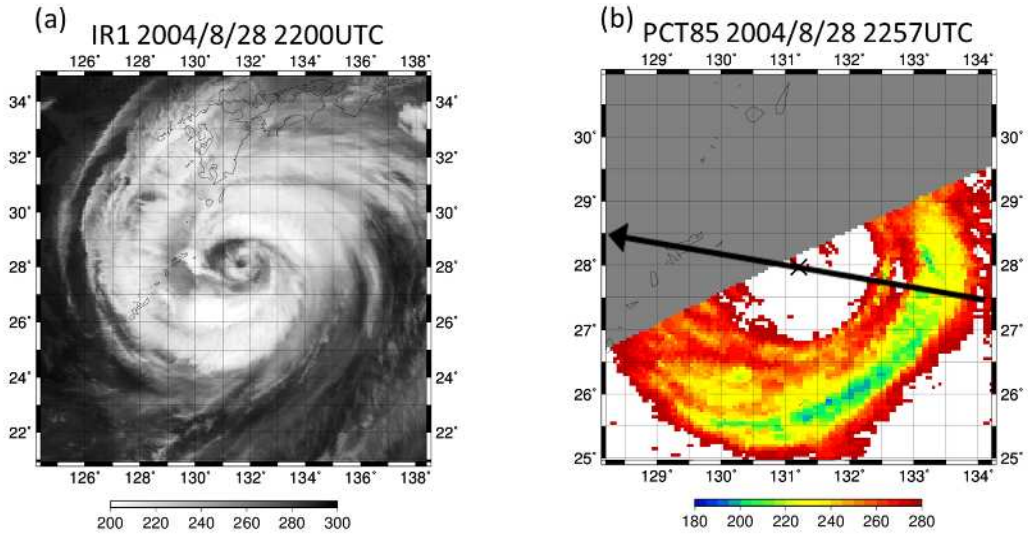

Figure 5. Satellite images of TC Chaba (0416). (a) GOES-9 infrared image at 2200 UTC 28 August 2004. (b) PCT85 at 2257 UTC 28 August 2004. The area of missing data coverage is shown in gray. The X and the arrow in the panel denote the TC center and the direction of movement, respectively.

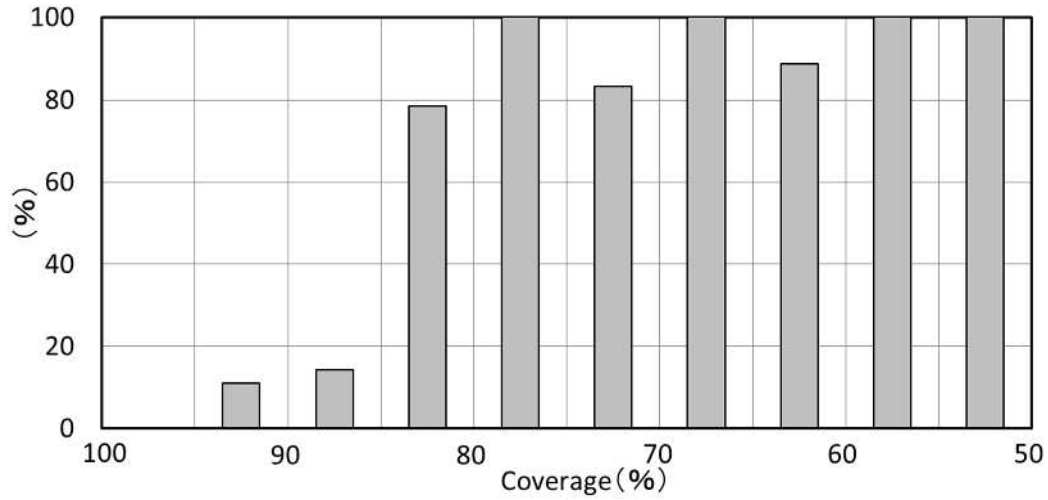

Figure 6. Ratios of potential misclassification due to a lack of TB coverage in the TC region. Gray bars denote percentages for cases with large estimation errors (> 10 m/s).

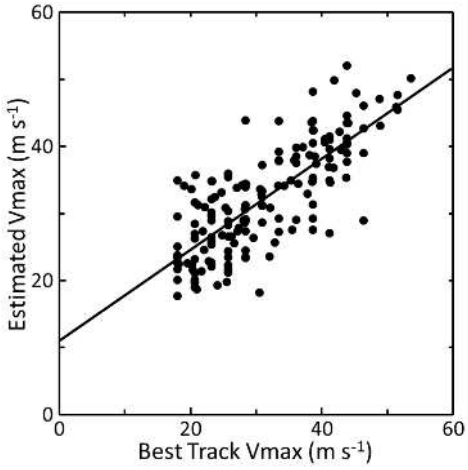

Figure 7. Scatter plot and regression line for the best track Vmax and estimated Vmax values for cases with data coverage complement.

4. Case studies

This section details estimates of maximum TC wind speeds for several cases in comparison with speeds estimated using the Dvorak technique and those in the best track data. CI numbers are operationally analyzed by JMA and converted into maximum wind speeds based on the table proposed by Koba et al. (1990). The resultant maximum wind speed is defined as an estimate based on the Dvorak technique.

Figure 8 shows time-series plots of maximum winds for TC Meari (1105) as a well-estimated example. PCT98 distribution for several selected cases is shown in Figs.

9a–c. It should be noted that this TC was accompanied by relatively weak convection even during its mature stage.

Figure 9b (1539 UTC 24 June 2011) shows a case in which a data coverage complement was applied. The coverage is about 87% within 2° of the TC center. The maximum wind speed in the best track data is 31.11 m/s, the estimate based on the Dvorak technique is 25.55 m/s, and that based on the proposed method is 30.9 m/s (Fig. 8). The difference between the estimate made with the proposed method and the best track wind maximum is smaller than that between the Dvorak estimate and the wind maximum despite a lack of TB data, suggesting that the complement procedure works well in this case.

The second example is TC Conson (1002) shown in Fig. 10. The maximum wind speed is significantly overestimated as 40.03 m/s in the early stage of development at 0058 UTC 12 July 2010, when the maximum wind speed based on the best track data was 18.87 m/s. In this case, the TC has a distinct eye and asymmetric TB distribution (Fig. 11a), and is classified into CL6. There is also an area with very low PCT85 values near the TC center. In Table 2, P_6 for CL6 is PCT85_MIN_C025A, and is considered to be the primary factor behind this overestimation. In general, estimation using the proposed method is relatively less accurate for the early stage of TC development. This may be partly because the convective system of the TC is poorly organized at this stage and may be classified into the wrong cluster. When the regression equation for CL1 is applied to the above-mentioned overestimation case for 0058 UTC 12 July 2010, the maximum wind speed is estimated as 29.39 m/s. This apparent improvement suggests that the overestimation may stem partially from misclassification.

At the next observation time (1550 UTC 12 July 2010, Fig. 11b), although the classification is again CL6, the estimate obtained using the proposed method is almost equal to that of the Dvorak technique. This consensus of the two estimates strongly supports the final analysis of TC intensity.

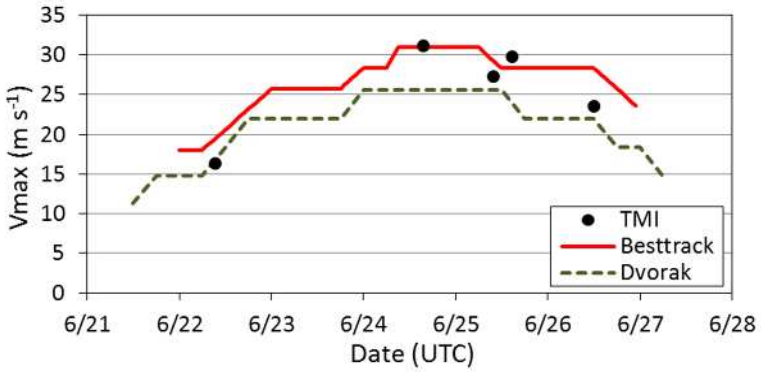

Figure 8. Time-series plots of estimated maximum wind speed for TC Meari (1105). The solid red line, the dashed green line and the dots denote maximum wind speed in the best track data, estimates based on the Dvorak technique, and those based on the proposed method, respectively.

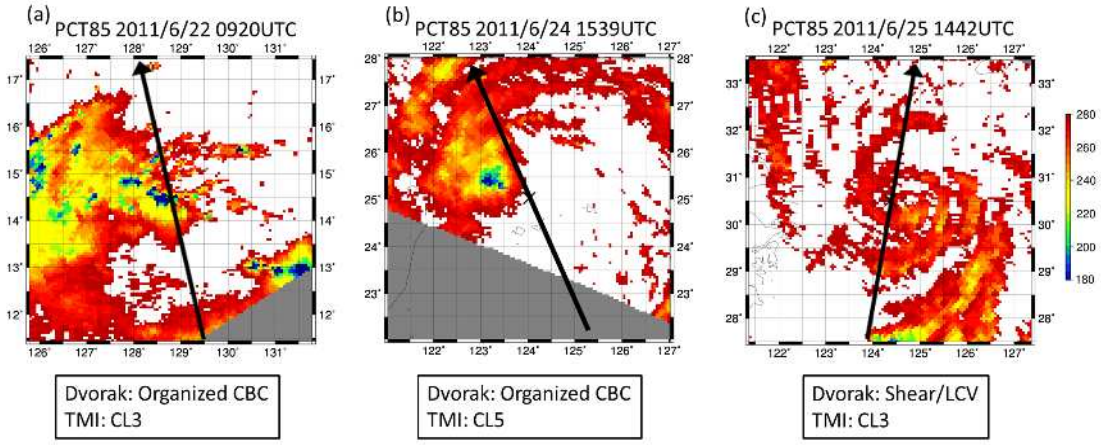

Figure 9. PCT85 distribution for TC Meari (1105) (a) at 0920 UTC 22 June 2011, (b) at 1539 UTC 24 June 2011, and (c) at 1442 UTC 25 June 2011. The X and the arrow in each panel denote the TC center and the direction of movement, respectively. The cloud pattern of the Dvorak technique and the cluster number of the proposed method are also noted under each panel.

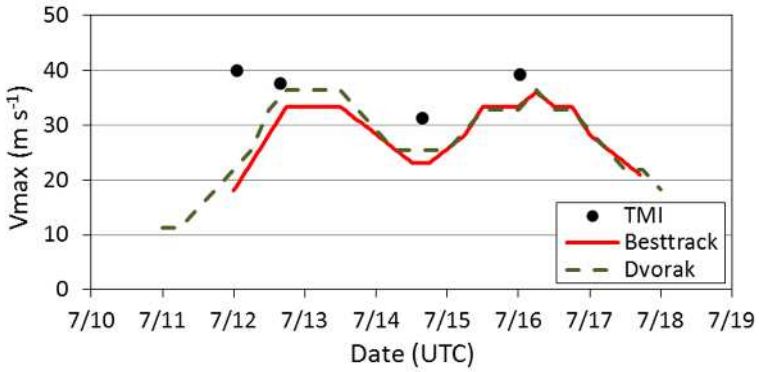

Figure 10. Same as Fig.8, but for TC Conson (1002).

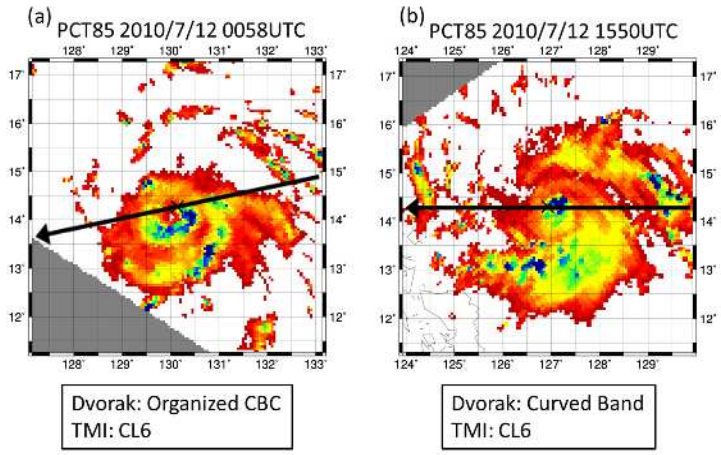

Figure 11. Same as Fig. 9, but for TC Conson (1002), (a) at 0058 UTC 12 July 2010 and (b) at 1550 UTC 12 July 2010.

5. Summary and remarks

In this study, a TC intensity estimation method using TRMM/TMI TB data was developed based on the technique proposed by HN07 taking the variety of TB distribution into account. TCs observed under the TRMM from 1998 to 2008 were classified into 10 clusters using the k-means method, and a regression equation for each cluster was defined using the maximum wind speed of the best track data as the dependent variable.

Estimated maximum wind speeds were verified for observed TC cases between 2009 and 2012 in comparison with maximum wind speeds based on the JMA best track data.

The results showed a bias of almost 0 m/s and a RMSE of 6.26 m/s, which is comparable to that of the Dvorak technique.

Maximum TC wind speeds estimated using this method are referenced by the RSMC Tokyo-Typhoon Center as supplementary information for operational TC intensity estimation. As TRMM/TMI data are not available until several hours after observation, operational TC intensity estimation primarily depends on the Dvorak technique using MTSAT imagery. This estimation method is used for confirmation and correction of operational estimates and for the best track analysis.

References

Dvorak, V. F., 1975: Tropical cyclone intensity analysis and forecasting from satellite imagery. *Mon. Wea. Rev.*, **103,** 420 – 430.

Dvorak, V. F., 1984: Tropical cyclone intensity analysis using satellite data. NOAA Tech. Rep. NESDIS 11, NOAA.

Hoshino, S. and T. Nakazawa, 2007: Estimation of tropical cyclone's intensity using TRMM/TMI brightness temperature data. *J. Meteor. Soc. Japan*, **85,** 437 – 454 (http://dx.doi.org/10.2151/jmsj.85.437).

Kiku, T., 2011: Improvements of an estimation method of tropical cyclone's intensity using microwave satellite data, Meteorological College undergraduate thesis (in Japanese).

Kitabatake, N., S. Hoshino and T. Sakuragi, 2013: Estimation of tropical cyclone intensity taking asymmetric distribution of TRMM/TMI brightness temperature into account. *Pap. Meteor. Geophys.*, submitted (in Japanese).

Koba, H., T. Hagiwara, S. Osano and S. Akashi, 1990: Relationship between the CI-number and central pressure and maximum wind speed in typhoon (in Japanese). *J. Meteor. Res.*, **42,** 59 – 67.

Spencer, R. W., H. W. Goodman and R. E. Hood, 1989: Precipitation retrieval over land and ocean with the SSM/I: Identification and characteristics of scattering signal. *J. Atmos. Oceanic Technol.*, **6,** 254 – 273.

Yoshida, S., M. Sakai, A. Shouji, M. Hirohata and A. Shimizu, 2011: Estimation of tropical cyclone intensity using Aqua/AMSR-E data. *RSMC Tokyo – Typhoon Center Tech. Rev.*, No. 13.